Dielectric properties of Sb 2 O 3 -doped Ba Fe 12 O 19 ferrite

P. Brahma, S. Banerjee, and D. Chakravorty

Citation: Journal of Applied Physics **98**, 064103 (2005); doi: 10.1063/1.2058220
View online: http://dx.doi.org/10.1063/1.2058220
View Table of Contents: http://scitation.aip.org/content/aip/journal/jap/98/6?ver=pdfcov
Published by the AIP Publishing

Dielectric properties of Sb_2O_3-doped $BaFe_{12}O_{19}$ ferrite

P. Brahma[a)]
Netaji Subhas Open University, 1 Woodburn Park, Kolkata 700 020, India

S. Banerjee
Department of Physics, University of Calcutta, Kolkata 700 009, India

D. Chakravorty[b)]
Indian Association for the Cultivation of Science, Kolkata 700 032, India

(Received 27 October 2004; accepted 4 August 2005; published online 26 September 2005)

Dielectric measurements were carried out on specimens with compositions $BaO.(6-x)Fe_2O_3.x\ Sb_2O_3$ with x having values of 0.0, 0.025, 0.1, and 0.3. Sb_2O_3 doping increases the dielectric permittivity drastically. Two loss peaks of similar activation energies were observed. The analysis showed that these arose because of the presence of $Fe^{2+}-Fe^{3+}$ and $Sb^{3+}-Sb^{5+}$ pairs, respectively, in the system. The experimental data could be analyzed satisfactorily in terms of Cole-Cole relaxation formalism. The relaxation distribution parameter α was found to be much larger in the case of $Sb^{3+}-Sb^{5+}$ pair than that due to $Fe^{2+}-Fe^{3+}$ pair. © *2005 American Institute of Physics*. [DOI: 10.1063/1.2058220]

INTRODUCTION

Ferrites are technologically important ceramic magnetic material and find many applications[1] because they are inexpensive, stable, and have wide range of applications, e.g., in transformer cores, high-quality filters, and operating devices. The electrical conductivity and dielectric behavior in ferrites depend on many factors, such as preparation method, sintering temperature, and amount and type of substitution.[2,3]

Recently we had reported on the dc conductivity of the Sb-substituted $BaFe_{12}O_{19}$ ferrites.[4] Electrical conduction has been explained as arising due to the presence of both small polaron hopping between Fe^{2+}- and Fe^{3+}-ion sites and the bipolaron hopping between Sb^{3+}- and Sb^{5+}-ion sites. It is felt that dielectric measurements should exhibit interesting relaxation processes. These measurements are carried out and the results are reported in this paper.

EXPERIMENT

Barium hexaferrite with the composition $BaO(6-x)Fe_2O_3.x\ Sb_2O_3(x=0,0.025,0.1,0.3)$ was prepared by the conventional ceramic route. Analytical Reagent (AR) grade $BaCO_3$, Fe_2O_3, and Sb_2O_3 were used as starting materials for the preparation of polycrystalline Sb_2O_3-doped barium hexaferrites. Stoichiometric mixture of the raw materials was thoroughly ground in acetone in an agate vessel for 2 h. Pellets with approximate diameter of 1 cm and thickness of 2–3 mm were made by cold pressing the powder obtained as above using a pressure of 5 tons/cm^2. The pellets were sintered at 1523 K in an electric furnace. Intermediate grinding and sintering were done after every 6 h heat treatment to ensure maximum conversion to barium hexaferrite. The crystalline phases present in the sintered specimens were determined from the x-ray-diffraction patterns taken on a Rich and Seifert 2000 P diffractometer using Cr $K\alpha$ radiation. The diffractogram obtained in the case of the sample with $x=0.025$ is shown in Fig. 1. Such diffraction patterns were obtained for all the samples studied here. It was found that all prepared samples had single phase M-type hexagonal structure.[5] The sample bulk density was measured and found to be more than 85% of the theoretical density (5.2 gm/cc) for all the samples. The amount of iron and antimony in different oxidation states was determined by a wet chemical analysis. The details of the chemical analysis have been reported earlier.[4] The dielectric measurements of ferrites in the frequency range of 1.5 kHz–10 MHz were carried out by an impedance analyzer (4192 ALF) in the temperature range of 120–300 K. The temperature was measured by a copper-constantan thermocouple placed close to the sample. The temperature was controlled with an accuracy of ±1 K using an Indotherm temperature controller. The sample was made

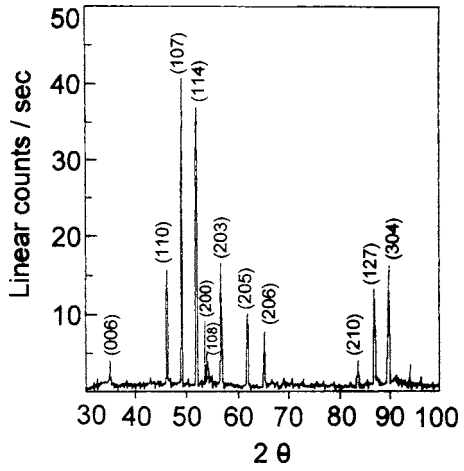

FIG. 1. X-ray diffractogram of a sample of composition $BaO.5.975\ Fe_2O_3.0.025\ Sb_2O_3$.

[a)]On leave from Physics Department, Gurudas College, Kolkata 700 054, India.
[b)]Electronic mail: mlsdc@mahendra.iacs.res.in

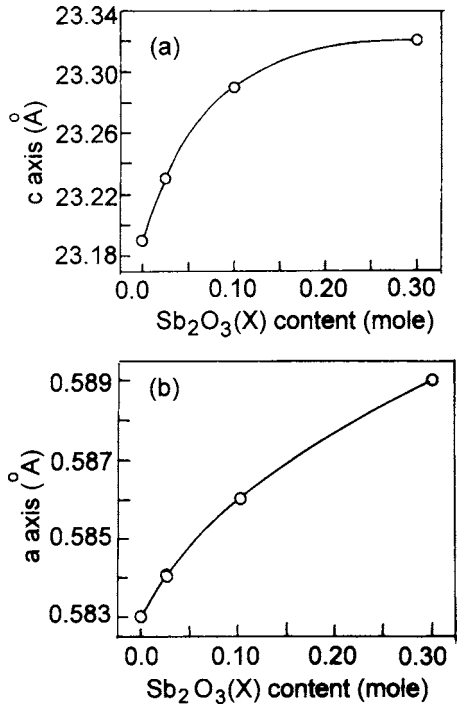

FIG. 2. Variation of lattice parameters of ferrite specimens as a function of Sb_2O_3 content. (a) parameter a and (b) parameter c.

in the pellet form of 1 cm diameter described as above for the capacitance C and dissipation factor (D) measurements.

The real (ε_1) and imaginary (ε_2) parts of the dielectric permittivity were estimated after subtracting the dc loss contribution from the measured dissipation factor.

RESULTS AND DISCUSSION

Figure 1 is the x-ray diffractogram obtained for the composition $BaO.(5.975)Fe_2O_3.(0.025)Sb_2O_3$. X-ray diffractograms of all the samples show the intensity peaks for the barium hexaferrite phases. No extra peaks are observed. These patterns confirm that the antimony oxide has formed a solid solution with barium hexaferrite. This conclusion is further substantiated by our earlier report on the magnetic characterization of barium hexaferrite doped with antimony oxide.[5]

Lattice parameters (a,c) of the ferrite specimens were determined from the d_{hkl} values extracted from the diffraction peaks (107) and (114). Figures 2(a) and 2(b) represent the variation of a (Å) and c (Å) parameters as a function of $Sb_2O_3(x)$ content (mole). The values of both the cell parameters of the barium hexaferrite structure increase as the Sb_2O_3 content is enhanced. It should be mentioned, however, that the ionic radius of Sb^{3+} ions is (0.9 Å) larger than that of Fe^{3+} ions (0.67 Å),[6] thus making a straight forward substitution difficult from the crystal chemistry point of view. The ionic radius of Sb^{5+} ion being 0.62 Å,[6] it is likely that some of the Fe^{3+} sites are occupied by Sb^{5+} ions thereby reducing the distortion energy of the lattice. A chemical reaction can be envisaged as follows:

$$Sb^{3+} + 2Fe^{3+} \rightarrow Sb^{5+} + 2Fe^{2+}. \quad (1)$$

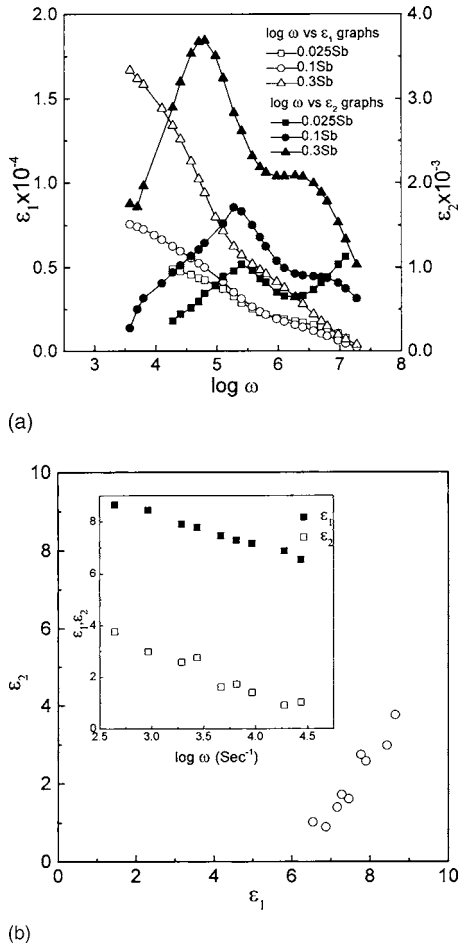

FIG. 3. (a) Variation of ε_1 and ε_2 as a function of frequency for different doped specimens. (b) Variation of ε_1 and ε_2 as a function of frequency for different undoped barium hexaferrite.

Chemical analysis investigation of these compounds has indeed shown the existence of Sb^{5+} ions in them. Experimental details along with the results of the chemical analysis have been reported earlier by the present investigators.[4]

The results of the dielectric measurements obtained at room temperature on the ferrite series are shown in Fig. 3(a). Figure 3(b) shows the real and imaginary parts of dielectric permittivity for the undoped barium hexaferrite. The values of ε_1 and ε_2, of ferrite samples, are drastically modified by a factor of $\sim 10^4$ when Sb_2O_3 is incorporated in the composition system. It is very interesting to note that even for a very small amount of doping (0.025 mole) three-order enhancement of dielectric permittivity (ε_1) has been observed.

Figure 3(a) shows a normal behavior of dielectric permittivity as a function of frequency at room temperature for all compositions of ferrite, where permittivity decreases with increasing frequency. Dielectric loss (ε_2) spectra show two peaks, as shown in Fig. 3(a). The peaks shift towards high-frequency region with increasing temperature as shown in Fig. 4 for the composition $x=0.3$.

The dielectric relaxation takes place when the jumping frequency of the electric charge carrier becomes approximately equal to that of external applied ac electric field. Two loss peaks can be assigned to electric dipole pairs constituted by Fe (Fe^{2+},Fe^{3+}) and Sb (Sb^{3+},Sb^{5+}) ions, respectively, as

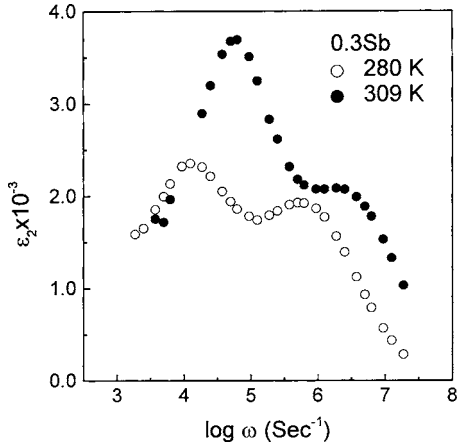

FIG. 4. Variation of ε_2 as a function of frequency at different temperatures for specimen of composition $BaO.5.7\ Fe_2O_3.0.3\ Sb_2O_3$.

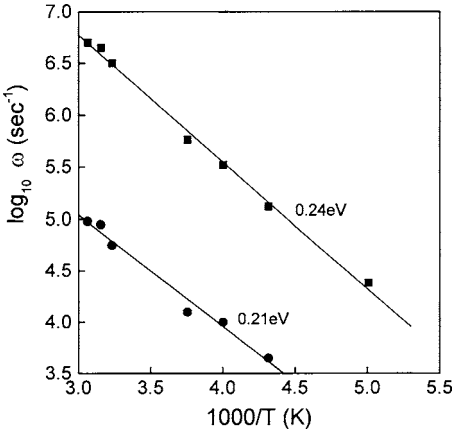

FIG. 5. Log_{10} (frequency at loss maximum) vs $1/T$ for the two relaxation processes in the case of specimen of composition $BaO.5.7\ Fe_2O_3.0.3\ Sb_2O_3$. (●)-$\omega_l$, (■)-$\omega_h$.

we recently concluded from dc electrical measurements.[4] Low- and high-frequency relaxation peaks (ω_l, ω_h) were used to calculate the corresponding relaxation times (τ_l, τ_h) using the following standard relation:

$$\omega_i \tau_i = 1. \tag{2}$$

The relaxation time is controlled by the following relation:

$$\tau_i = \tau_{i0} \exp(E_i/kT), \tag{3}$$

where k is the Boltzmann constant and E_i's are the activation energies for the dielectric relaxation. We estimated activation energies for the two relaxation processes as shown in Fig. 5 by a least-square fitting of data points to a straight line for the ferrite composition $x=0.3$.

Activation energies estimated for the other compositions along with the preexponential constants τ_i and dc activation energies are shown in Table I. The activation energies for dc conduction which are shown in the last column of Table I were found to be in reasonable agreement with those obtained from dielectric relaxation measurements. This suggests that the hopping mechanisms are the same in both cases.

Figure 6 shows complex permittivity plot for the compositions $x=0.025$ and 0.3 mole Sb_2O_3 measured at 234 and 232 K, respectively. This is typical for all the samples over the measured temperature range. Two semicircular arcs again suggest that two dielectric relaxation processes are operative as stated earlier.

Various relaxation models, such as the Debye relaxation,[7] the Cole-Cole,[8] the Davidson-Cole relaxation,[9] and the Havriliak-Negami[10] relaxation, are known for the analysis of the frequency-dependent properties of dielectric materials.

We choose Cole-Cole relaxation process [Eq. (4)] for analyzing dielectric permittivity data in the present ferrite series

$$\varepsilon^*_{ii}(\omega) = \varepsilon_{\infty i} + \frac{\varepsilon_{0i}\varepsilon_{\alpha i}}{1 + (j\omega\tau_i)^{1-\alpha_i}}, \tag{4}$$

where ε_{si}'s are the real part of permittivity when ω approaches zero, $\omega_{\infty i}$'s are the real part of permittivity when ω approaches infinity (i.e., when ω is large for the relaxation process under investigation) and τ_i's are the permittivity relaxation times corresponding to low- and high-frequency relaxation processes, and α_i's are the distribution parameters. The experimental ε_1 and ε_2 data obtained at different frequencies for the Sb- substituted barium hexaferrites ($x=0.025$ and 0.3) were least square fitted to Eq. (4) using ε_{0i}, $\varepsilon_{\alpha i}$, and α_i as parameters. Two arcs of circles were fitted to the data. The theoretically fitted curves are shown in Fig. 6 by the solid lines. The fitting to experimental data is found to be satisfactory. The values of different parameters as extracted by this procedure for different samples are summarized in Table II. Variation of distribution parameters (α_i) with antimony doping is shown in Fig. 7. We can draw the following conclusions from the parameters listed in Table II.

(i) Distribution parameters (α) at low- and high-frequency regimes are temperature independent.

TABLE I. Values of activation energies (ac values).

Sb present	ac activation (eV) low frequency	τ_0 (s) from low-frequency peak	ac activation (eV) high frequency	τ_0 (s) from high-frequency peak	dc activation energy (eV)
0.025	0.19	4.8×10^{-9}	0.20	4.4×10^{-11}	0.17±0.02
0.1	0.16	1.2×10^{-8}	0.19	1.1×10^{-10}	0.10±0.03
0.3	0.21	5.1×10^{-9}	0.24	3.6×10^{-11}	0.14±0.04

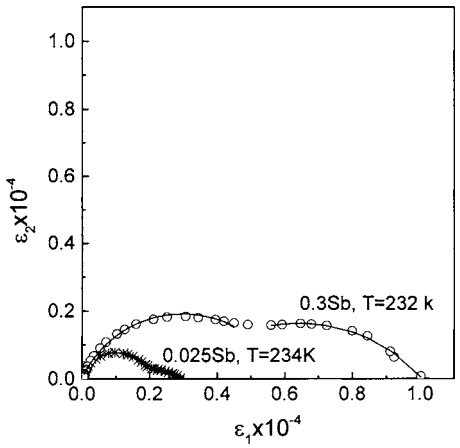

FIG. 6. Complex permittivity plot for compositions with Sb_2O_3 contents of 0.025 and 0.3 mole, respectively.

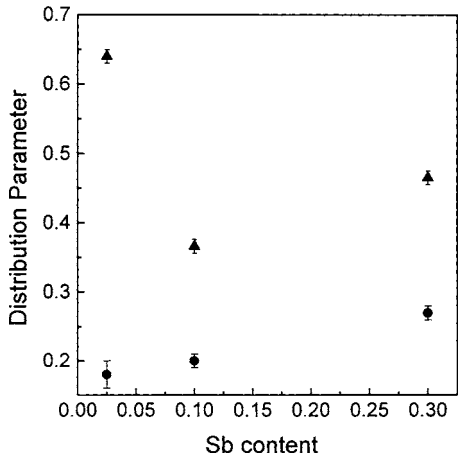

FIG. 7. Variation of distribution parameter α as a function of antimony doping. (■)-τ_h, (▲)-τ_l.

(ii) α corresponding to the high-frequency region is smaller than that corresponding to the low-frequency region.

The above conclusions are consistent with the data presented in Fig. 7.

Finally after comparing dielectric behavior of doped ferrite materials with undoped ferrite [Fig. 2(b)]; low- and high-frequency relaxations can be ascribed to (Sb^{3+}–Sb^{5+}) and (Fe^{2+}–Fe^{3+}) dipole pairs, respectively. The ion-pair Sb^{3+}–Sb^{5+} contributed a much larger polarizability to the material (viz., permittivity $\sim 10^3$) than the Fe^{2+}–Fe^{3+} pair. This is consistent with the charges involved and their separation. It is interesting to note that the low-frequency relaxation process is more Debye type than the high-frequency one. This is ascribed to the fact that there is much less distribution of relaxation times in the case of the low-frequency relaxation than the high-frequency one. This arises because the doping level being rather small, the distribution of separation distances between Sb^{3+} and Sb^{5+} ions will be rather narrow which will restrict the distribution of relaxation times.

The main conclusions have been the identical values of activation energies obtained for both the relaxation mechanisms, viz., at low and high frequencies, respectively. As explained in the previous paragraph these peaks are assigned to Sb^{3+}–Sb^{5+} and Fe^{2+}–Fe^{3+} pairs, respectively. For the former the bipolaronic model can be invoked which gives as the activation energy the expression[5]

$$W_1 = W_M - \frac{2e^2}{\pi\varepsilon\varepsilon_0 R_p}, \tag{5}$$

where W_M is the potential energy associated with a defect site, ε is the dielectric constant of the medium, ε_0 is the free space permittivity, and R_p is the hopping distance. Substituting W_M=0.73 eV (Ref. 5) and W_1=0.19 eV (Table I) we calculate from (5) a value of R_p=1.8 nm. This is of the same order as the value of the crystallographic parameter c [see Fig. 2(b)]. This means Sb ions are located at sites along the c axis of the ferrite crystal. We have also calculated from the expression for small polaron hopping energy[5]

$$W = \frac{e^2}{4\varepsilon_p r_p}, \tag{6}$$

a value of $\varepsilon_p \sim 7.0$ after substituting in Eq. (6) W=0.17 eV and r_p=3.14 Å. This value is in reasonable agreement with the measured value of dielectric permittivity for the material at high frequencies.

From this discussion we conclude that the observed experimental results arise due to the presence of Sb^{3+}–Sb^{5+} and Fe^{2+}–Fe^{3+} pairs, respectively.

TABLE II. Parameters for Cole-Cole fitting.

		High-frequency arc				Low-frequency arc			
Sample	T (K)	ε_{0h}	$\varepsilon_{\alpha h}$	τ_h	α_h	ε_{01}	$\varepsilon_{\alpha 1}$	τ_1	α_1
	266	2.05×10^3	12	3.5×10^{-7}	0.14	4.09×10^3	0.77×10^3	1.53×10^{-5}	0.62
0.025	234	2.08×10^3	12	9.93×10^{-7}	0.18	2.95×10^3	0.79×10^3	4.14×10^{-5}	0.64
	205	2.10×10^3	12	4.47×10^{-7}	0.19	2.70×10^3	1.30×10^3	2.04×10^{-5}	0.62
	252	2.60×10^3	12	9.77×10^{-7}	0.20	6.85×10^3	1.03×10^3	3.31×10^{-5}	0.37
0.1	190	2.47×10^3	12	1.12×10^{-5}	0.21	5.05×10^3	1.09×10^3	2.75×10^{-4}	0.38
	309	7.04×10^3	12	3.16×10^{-7}	0.28	1.81×10^3	2.15×10^3	1.78×10^{-5}	0.46
0.3	132	5.96×10^3	12	7.58×10^{-6}	0.27	1.01×10^3	2.74×10^3	2.24×10^{-4}	0.47

ACKNOWLEDGMENT

One of the authors (D.C.) thanks Indian National Science Academy, New Delhi for the award of a Senior Scientist position.

[1]J. Kulikowski, J. Magn. Magn. Mater. **41**, 56 (1984).
[2]A. A. H. El Hiti, M. A. Ahmed, M. M. Mossad, and S. M. Attia, J. Magn. Magn. Mater. **150**, 399 (1995).
[3]A. M. Abo El Ata and M. A. Ahmed, J. Magn. Magn. Mater. **208**, 27 (2000).
[4]P. Brahma, S. Banerjee, S. Chakraborty, and D. Chakravorty, J. Appl. Phys. **88**, 6526 (2000).
[5]P. Brahma, A. K. Giri, D. Chakravorty, H. Tiwari, and D. Bahadur, J. Magn. Magn. Mater. **102**, 109 (1991).
[6]W. D. Kingery, *Introduction to Ceramics* (Wiley, New York, 1967), p. 109.
[7]P. Debye, *Polar Molecules* (Dover, New York, 1929).
[8]K. Cole and R. H. Cole, J. Chem. Phys. **9**, 341 (1941).
[9]W. D. Davidson and R. H. Cole, J. Chem. Phys. **19**, 1484 (1951).
[10]S. Havriliak and S. Negami, Polymer **8**, 161 (1967).